Biogeosciences Discuss., 10, 2345–2375, 2013
www.biogeosciences-discuss.net/10/2345/2013/
doi:10.5194/bgd-10-2345-2013

Biogeosciences Discussions Open Access

Taking nature into lab: biomineralization by heavy metal resistant streptomycetes in soil

E. Schütze[1], A. Weist[1], M. Klose[1], T. Wach[1,5], M. Schumann[1,5], S. Nietzsche[2], D. Merten[3], J. Baumert[4], J. Majzlan[5], and E. Kothe[1]

[1]Microbial Communication, Institute of Microbiology, Friedrich Schiller University, Jena, Germany
[2]Centre for Electron Microscopy, Clinical Centre, Friedrich Schiller University, Jena, Germany
[3]Applied Geology, Institute for Earth Sciences, Friedrich Schiller University, Jena, Germany
[4]Mineralogy, Institute for Earth Sciences, Friedrich Schiller University, Jena, Germany
[5]Biogeochemical Processes, Max Planck Institute for Biogeochemistry, Jena, Germany

Received: 11 December 2012 – Accepted: 18 January 2013 – Published: 11 February 2013

Correspondence to: E. Kothe (erika.kothe@uni-jena.de)

Published by Copernicus Publications on behalf of the European Geosciences Union.

Abstract

Biomineralization by heavy metal resistant streptomycetes was tested to evaluate the potential influence on metal mobilities in soil. Thus, we designed an experiment adopting conditions from classical laboratory methods to natural conditions prevailing in metal-rich soils with media spiked with heavy metals, soil agar, and nutrient enriched or unamended soil incubated with the bacteria. As a result, all strains were able to form struvite minerals on tryptic soy broth (TSB) media supplemented with $AlCl_2$, $MnCl_2$ and $CuSO_4$, as well as on soil agar. Some strains additionally formed struvite on nutrient enriched contaminated and control soil, as well as on metal contaminated soil without addition of media components. In contrast, switzerite was exclusively formed on minimal media spiked with $MnCl_2$ by four heavy metal resistant strains, and on nutrient enriched control soil by one strain. Hydrated nickel hydrogen phosphate was only crystallized on complex media supplemented with $NiSO_4$ by most strains. Thus, mineralization is a dominant property of streptomycetes, with different processes likely to occur under laboratory conditions and sub-natural to natural conditions. This new understanding may be transferred to formation of minerals in rock and sediment evolution, to ore deposit formation, and also might have implications for our understanding of biological metal resistance mechanisms. We assume that biogeochemical cycles, nutrient storage and metal resistance might be affected by formation and re-solubilization of minerals like struvite in soil at microscale.

1 Introduction

Biomineralization can be seen as formation of crystals intracellularly or in the extracellular matrix of organisms (Adele, 1998). A more detailed definition implies that biomineral deposition requires, or is associated to, a living organism (Veis, 2003). Two mechanisms are described according to the contribution of the involved organisms (Konhauser and Riding, 2012), namely biologically induced, passive and microbially

controlled, active biomineralization. The properties of the latter crystals, down to the minutiae, are meticulously controlled (Konhauser and Riding, 2012; Weiner and Dove, 2003). Consequently, interactions between living organisms and their abiotic environment need to be taken into account to understand the physico-chemical processes at or near the Earth's surface coupling biosphere and geosphere evolution (Cappellen, 2003; Schütze and Kothe, 2012).

Almost all groups of minerals, including carbonates, phosphates, sulfates and sulfides, arsenates, silica, chlorides, fluorides, oxides, hydroxides and Fe-Mn-oxides are known to be produced by biomineralization. Phosphates are the main class beside iron oxides and represent about 25 % of the biogenic minerals which are usually formed in a biologically controlled fashion. Exceptions are struvite and brushite which are known to be formed biologically induced (Konhauser and Riding, 2012; Weiner and Dove, 2003). Struvite is a well-known (bio)mineral occurring in human urinary sediments and as kidney stones with a nominal composition $MgNH_4PO_4 \cdot 6H_2O$ (Le Corre et al., 2007a; Stefov et al., 2005; Lee et al., 2003). It shows a high potential for industrial use since phosphate and ammonia can be precipitated from wastewaters (Le Corre et al., 2007a; Lee et al., 2003; Kofina and Koutsoukos, 2005). The solubility of struvite is known to be low (0.2 $g\,L^{-1}$ in water), although it is known to be entirely citrate soluble (Hesse et al., 1989).

The influence of microorganisms on struvite mineralization was tested in a number of studies (Rivadeneyra et al., 1992; Kamnev et al., 1999; Stefov et al., 2005; Ben Omar et al., 1998; Da Silva et al., 2000).These works showed that 58.3 % of the tested bacteria isolated from soil and fresh water were able to produce struvite, including strains of the genera *Acinetobacter*, *Arthrobacter*, *Bacillus*, *Corynebacterium*, *Kurthia*, *Staphylococcus*, *Desulfobrio*, *Listeria*, *Proteus*, *Yersinia*, *Escherichia* (and other members of the family of Enterobacteriaceae), *Ureaplasma*, *Aeromonas*, *Alcaligenes*, *Micrococcus, Murraya*, *Plesiomonas*, *Myxococcus* and *Brucella*. Struvite biomineralization is suggested to be linked to the release of ammonium from organic matter, either by decomposition of organic material or by urea hydrolysis through microbial urase

activity (Rivadeneyra et al., 1999). Other processes have been postulated, because urease-negative bacteria have also been shown to be capable of struvite mineralization. Additionally, some urease-positive strains did not induce crystallization of struvite, even though high concentrations of ammonia were produced (Rivadeneyra et al., 1990, 1999).

An important biogeochemical factor influencing struvite formation is pH,with struvite formation between pH 5 and 9.5, increasing above 8.8 (Doyle et al., 2000; Pérez-García et al., 1989; Prywer and Torzewska, 2009; Da Silva et al., 2000). In a pilot-scale reactor experiment, small variations of pH, concentration of Mg or Ca, and the retention time had a significant impact on struvite crystal characteristics and/or production (Le Corre et al., 2007b). CO_2 degassing suppressed struvite biomineralization (Saidou et al., 2009).

A new phase isostructural with struvite, in which Mg is replaced by Ni (although Mg had been present in the media) has been reported to be formed by heavy metal resistant *Strepromyces acidiscabies* E13 (Haferburg et al., 2008). This phase has a nominal composition $(NH_4)Ni(PO_4) \cdot 6H_2O$ and had prior to this study been known only from technical production.

Although intracellular binding of nickel to polyphosphate bodies is reported for *Staphylococcus aureus* (Gonzalez and Jensen, 1998), no further biomineralization of nickel phosphates is described in literature. However, microbially enhanced chemisorption of heavy metals into pre-existing minerals has been reported for Ni (Basnakova et al., 1998).

In comparison to uncontaminated soils, heavy metal contaminated soils show evidence for prevalence of Gram-positives (Schütze and Kothe, 2012). Thus, streptomycetes were investigated to study biomineralization in soils to understand the processes involved, as well as the ecological relevance of mineral formation, in treatments mimicking sub-natural to natural conditions. To our knowledge, natural and artificial soil extract was used in one example so far to determine calcite biomineralization in

vitro (Párraga et al., 2004). Hence, our approach leads to a deeper insight into natural conditions under which different minerals can be formed.

2 Material and methods

2.1 Strains and growth of bacteria

Extremely heavy metal resistant streptomycetes (Schmidt et al., 2008) isolated from the former uranium mining site WISMUT, Ronneburg, Germany, were used to study biomineralization on heavy metal supplemented media, soil agar and directly in soil from different sampling sites.

S. chromofuscus P10A-4, *S. mirabilis* P10A-3, *S. mirabilis* K7A-1, *S. prunicolor* P6A-1, *S. naganishii* P9A-1, *S. mirabilis* P16B-1, *S. chromofuscus* P4B-1, *S. acidiscabies* E13 and heavy metal sensitive control strain *S. lividans* TK23 were cultured on agar plates containing oatmeal media (20 g oatmeal, 2 g glucose, 1.8 % agar) for spore production. Spore suspensions were harvested after 7 days of growth at 28 °C and purified by filtration through absorbent cotton using distilled water (Kieser et al., 2000). CFU was determined on actinomycete minimal (AM) medium (Schmidt et al., 2008). For preparation of dead biomass (control), AM or TSB medium (tryptic soy broth, Bacto) in 100 mL test tubes was inoculated and incubated 7 days at 28 °C. Culture aeration started 48 h after inoculation by shaking at 160 rpm. The mycelium was harvested (4000 rpm, 4 °C, 30 min, Megafuge 1.OR Heraeus), washed with distilled water, and autoclaved.

2.2 Soil samples and analysis of soil

The soils used for these experiments were a non-contaminated control (C), contaminated test field soil (M1) and a highly contaminated soil from a creek bank (M2). Heavy metal contaminated soil samples were collected at the former uranium mining site

WISMUT, Ronneburg, Germany, from our testfield (M1) area and sample site K7 (M2) from the bank of the creek Gessenbach (Schmidt et al., 2005). Control soil was taken from a central park, "Paradies" (C), Jena, Germany (GPS 44709773, GK 5642870). All soil were dried at 30 °C and sieved to a maximum grain size of 2 mm.

For the determination of water holding capacity (WHC), 100 g of soil were transferred into a glass drip and dowsed with 100 mL of distilled water. After 24 h, the discharge was quantified and WHC was calculated. Sequential extraction was performed to assess the bioavailable fractions of mobile (F1) and specifically adsorbed (F2) metals (Zeien and Brümmer, 1989) using ICP-MS/ICP-OES (XSeries II, ThermoFisher Scientific, Bremen, Germany) and /ICP-OES (725 ES, Varian, Darmstadt, Germany).

For carbon (C), nitrogen (N) and sulfur (S) contents, soil was ground to a maximum grain size of < 63 µm. From each sample, 20 mg were transferred into tin capsules and mixed with tungsten trioxide. Analysis was performed using VarioEL (version F, ElementarAnalysesysteme GmbH) with sulfanilic acid (5 mg, without WO_3, C 41.61 %, N 8.09 %, H 4.07 %, S 18.51 %, O 27.71 %) and T100 (beech tree leaves: 28.5 mg, with WO_3, C 50.30 %, N 2.629 %, H 6.335 %, S 0.269 %) as standards.

2.3 Biomineralization experiments and characterization of minerals

Biomineralization experiments were performed under artificial, sub-natural and natural conditions on metal supplemented media (MSM), soil agar (SA) and nutrient-enriched soil (NES). Nutrient supply resulted from addition of AM or TSB.

For biomineralization under artificial conditions, metal-supplemented media (MSM) were used. Stock solutions of metals (sterilized by filtration) were added to the autoclaved media to final concentrations of 30 mM $NiSO_4$, 1 mM $CuSO_4$, 20 mM $MnCl_2$, 1 mM $AlCl_3$ and 20 mM $ZnSO_4$ mimicking the natural conditions at the metal conatminated test site. Petri dishes were inoculated in duplicates with 5 droplets of 3 µL spore suspension per strain. As a control, dead biomass was used in addition to plates not inoculated. All treatments were performed in triplicates.

To mimic subnatural and natural conditions, soil agar (SA content: 1 : 1, 1 : 5, 1 : 10; Schmidt et al., 2008) and nutrient enriched soil (NES prepared from 100 g autoclaved soil containing 1 mL media per gram soil (C, M1, M2) at final WHC of 50 %) were used. Control plates were prepared without the addition of any media components. Soil and soil agar was inoculated in plates in duplicates with 5 droplets of 3 µL spore suspension per strain, sealed with parafilm to avoid desiccation, and incubated at 28 °C for 56 days (MSM, SA) and 70 days (NES).

Microphotographs and semi-quantitative chemical analyses were acquired with a scanning electron microscopes (SEM, LEO-1450 VP/ Oxford-Link Isis or Zeiss Ultra Plus with a built-in energy-dispersive X-ray spectrometer). The acceleration voltage was 20 kV and the observation were done on air dried cultures after carbon coating. Electron microprobe analyses (EMPA) were performed with a Cameca SX50 instrument with an acceleration voltage of 20 kV and beam current of 20 nA. The cultures were dried at 80 °C, fixed on glass slides by self-adhesive label, coated with carbon and analyzed. Crystal structure of the biominerals was investigated with a X-ray diffractometer (Bruker AXS D8 Advance), employing Cu Ka radiation. The samples were powdered and smeared onto a zero-background silicon sample holder and scanned in the angular range of 5–80° 2θ, step size of 0.01° 2θ and dwell time of 2 s.

2.4 Microbial processes influencing geochemical parameters

Ammonification (colorimetrically using universal indicator, Unitest) and pH changes of the media (via pH probe noLab pH 720, WTW) were verified in liquid cultures after 10 days of growth at 28 °C and 160 rpm or on indicator plates containing 0.05 g bromothymol blue or 0.025 g methyl L^{-1} of media. Urease production was measured (Bioassay Systems) for extracellular (supernatant) and intracellular (crude extract of mycelium ground in liquid nitrogen, dissolved in sodium phosphate buffer 50 mM, pH 7.8, centrifugation 11,000 rpm, 4 °C, 20 min, Hettich) activity in AM media to mimic nutrient-poor conditions.

3 Results

3.1 Growth and crystal production under artificial conditions

All tested strains were able to grow on rich TSB and depleted mineral AM media. Addition of 1 mM metal salts to AM medium suppressed growth of the sensitive control strain *S. lividans* TK23, but also some of the heavy metal resistant isolates (Table 1). TSB supported growth with metal addition, even with the metal sensitive strain, in three of the five metals tested: Cu, Al and Mn. At least one metal at the concentration of 1 mM was tolerated in AM by each of the metal resistant isolates, with growth on AM with up to 4 of the 5 metals tested being observed with multi-metal resistant *S. mirabilis* P16B-1. For heavy metal supplemented plates, three different kinds of minerals could be detected: struvite on TSB without metal addition or with Al, Cu or Mn in all cases; nickel hydrogen phosphate was produced on nickel containing TSB by 6 of the metal resistant isolates; switzerite ($Mn_3(PO_4)_2 \cdot 7H_2O$) was found on AM plates containing Mn for 4 strains (Fig. 1).

The morphology of struvite was variable (Fig. 1a–f; Table 2) for different strains, biomineralization occurred not only on the colony surface, but also in the media close to the colony. Most common habitus of struvite is acicular, but the products also included radial aggregates of acicular crystals, platy crystals with a wedge-like outline, parallel intergrowths of subhedral crystals, or fine-grained aggregates (Table 2). Switzerite occured as fine-grained aggregates devoid of crystal forms.

3.2 Establishing conditions for sub-natural to natural conditions for biomineralization

To mimic field conditions, but still being easy-to-manipulate conditions, soil agar plates were chosen. In order to simulate natural conditions even better, soils were used directly, without the addition of agar, but instead adding nutrient solution to allow for better growth of the streptomycetes inoculated in the soil.

The soils used for these experiments were the non-contaminated control (C), contaminated test field soil (M1), and a highly contaminated soil from a creek bank (M2). The elemental analyses for these soils revealed that, albeit higher in bioavailable metal concentration (Fig. 2), M2 soil was intermediate in respect to C and N contents, while the test field soil was extremely deprived in carbon, nitrogen and sulfur (Table 3). In addition, phosphate was under detection limit in all soils for both mobile and specifically adsorbed fractions, while potassium and sodium were below detection limit in the specifically adsorbed fractions with different contents in the mobile fractions (see Table S1). Magnesium was present at elevated levels in C and M2 with more than $600\,\mu g\,g^{-1}$, while approximately $150\,\mu g\,g^{-1}$ were found in the nutrient-poor test field soil M1. Values for Ca and Mg have been lowest in M1 soil (F1 + F2: $362\,\mu g\,Ca\,g^{-1}$ soil, $137\,\mu g\,Mg\,g^{-1}$ soil) and highest in C soil (F1 + F2: $12078\,\mu g\,Ca\,g^{-1}$, $589\,\mu g\,Mg\,g^{-1}$ soil). As for the heavy metal load, M2 soil clearly showed the highest concentrations with additional contamination of Cd ($0.292\,\mu g\,g^{-1}$ mobile), Co ($2.391\,\mu g\,g^{-1}$ mobile), and U ($0.152\,\mu g\,g^{-1}$ mobile and $171\,\mu g\,g^{-1}$ specifically absorbed), while Fe, as well as Al, was highest in control soil.

3.3 Growth and crystal production under sub-natural conditions on soil agar (SA)

Sub-natural conditions were achieved by the use of soil agar with two different amounts of C, M1, or M2 soil at 1 : 5 and 1 : 1 soil contents in either rich TSB or minimal AM medium, respectively. As a control, water agar was used to which the soil was added. For the highly metal contaminated M2 soil, a third soil concentration of 1 : 10 was included. On all C soil agar plates, all strains grew, albeit without crystals being observed. On M1 and M2, formation of struvite was observed in some samples (Table 4) where mycelium was partly encrusted by struvite (Fig. 1g). Interestingly, small amounts of Mn were detected in the minerals formed by *S. mirabilis* P16B-1 on M2 soil by element mapping (Fig. 3b). This indicates that other metals can either be incorporated or sorbed to the surface of struvite. In comparison to the laboratory plate assays (MSM),

the availability of Ni or Mn did not lead to switzerite or nickel hydrogen phosphate formation.

3.4 Growth and production of crystals under natural conditions

To mimic natural conditions most similar to the original environment, soil was used for microcosms with and without addition of media components imitating fertilized soils. Again, all strains were able to grow on C soil with or without media components, as well as on TSB supplemented M1 and M2 soil. In general, the bacteria grew better on M2 soil than on M1 soil, most likely linking the higher intrinsic nutrition to growth. Surprisingly, the heavy metal resistant strains grew better on M2 soil without addition of any media components than on media supplemented soil, which might indicate that addition of mineral nutrient elements might lead to salt stress in the highly contaminated soil. Struvite and switzerite (Fig. 1i, j) were obtained from some of these nutrient enriched soil microcosms (Table 5). Specifically for the contaminated M1 soil, if growth occurred, crystallization of struvite could be verified in almost all cases.

4 Investigation of potential mechanisms for biomineralization

To determine factors involved in biologically-induced mineral formation, pH changes, ammonification and urease activity were tested. The shift of pH varied, with both positive and negative shifts, in a wide range. On TSB media, rather changes to alkaline conditions could be detected, while acidification was found to be associated with growth on AM (Table 6). Using indicator plates, diffusion of the acids produced on AM could be shown, which leads to a diffusion gradient in physico-chemical conditions linked to the bacterial metabolism (Fig. 4a). For TSB containing indicator plates, neutral to slightly alkaline pH in a close vicinity to the colony could be shown (Fig. 4b). Thus, alteration of pH strongly depends on media components, their buffer capacity and excreted metabolites. Ammonification could be revealed in liquid TSB medium for the

tested strains, while liquid AM medium did not allow for ammonium formation (Table 6). Hence, urease excretion was tested with AM grown cells. As a control, also intracellular urease levels were determined. Both intracellular and extracellular urease activity was shown for all tested strains (Fig. 5).

5 Discussion

Bacteria can contribute actively to geological processes in biogeochemical cycling, metal mobility, mineral transformation, decomposition, bioweathering, and soil and sediment formation (Gadd, 2010; Cappellen, 2003). With respect to heavy metal containing soils, resistance is a prerequisite for survival and contribution to biogeochemical processes. The strains *S. chromofuscus* P10A-4 and P4B-1, *S. mirabilis* K7A-1, P10A-3 and P16B-1, *S. naganishii* P9A-1 and *S. prunicolor* P6A-1 were previously tested for their metal resistance on minimal media containing different concentration of $NiCl_2$, $NiSO_4$, $AlCl_3$, $CdCl_2$, $CoCl_2$, $CuSO_4$ and $ZnSO_4$ (Schmidt et al., 2008). Here, we could show that all strains were able to form biominerals and that media influenced crystal formation. Indeed, all tested strains induced struvite formation under certain conditions, and two other, formerly not detected streptomycete biominerals, namely switzerite and nickel hydrogen phosphate could be produced on metal spiked plates. The formation of another phosphate containing mineral, Ni-struvite, had been reported before for *S. acidiscabies* E13 (Haferburg et al., 2008). In that case, however, $NiCl_2$ instead of the sulfate was used, which might have resulted in conditions favoring the Ni-struvite precipitation.

The struvite crystals formed differed in macroscopic appearance, which has been described earlier for struvite biominerals with shapes from planar, X-shapped (McLean et al., 1991), hemimorphic, coffin-lid, twining (Prywer and Torzewska, 2010), to complex superstructures like tetragonal bipyramids or prismatic structures (Chen et al., 2010). Time, and especially pH, have been reported to exert a major impact on resulting crystal shape (Chen et al., 2010; Prywer and Torzewska, 2009, 2010). In addition, for the

synthetic production of struvite, it could be shown that the morphology of the crystals was influenced by the initial concentration of Mg in solution, with increasing Mg concentrations leading to more frequent orthorhombic shape and biger size of the crystals. Ca ions also showed a significant impact on size, shape and purity of the product recovered (Le Corre et al., 2005), which is of importance specifically in our trials where the soils contained different concentrations of Ca as well as other metals. The Mg contents led to Ca : Mg ratios of 2.6 : 1 for M1 soil, 6.4 : 1 for M2 soil and 20 : 1 for C soil. It has been shown by Le Corre et al. (2005) that increasing Ca concentration reduced the crystal size and also inhibited struvite formation at high Ca loads. In these laboratory based investigations, it has been found that Ca : Mg ratios of less than 1 inhibited struvite formation and favored formation of amorphous calcium phosphate instead. The high Ca : Mg ratios up to 20 : 1 and the fact that struvite was formed nevertheless indicate that in soil, biomineralization of struvite is influenced by other parameters, most likely depending on the bacterial activities in our inoculated samples.

In one instance, manganese incorporation or adsorption to struvite could be shown. The same effect has been published for metal addition to stored urine which resulted in co-precipitation of Cd, Cu and Pb with switzerite, while Co, Cr and Ni as well as As were not incorporated (Ronteltap et al., 2007).

Urease activity was detected both intracellularly and exctreted. Since the presence of urea is unlikely in soil without addition of manure, the induction of enzyme expression is likely dependent on other inducers not yet known. In accordance to struvite biomineralization having been suggested to be linked to the release of ammonium from organic matter by decomposition of organic material through microbial urease activity (Rivadeneyra et al., 1999), urease activity could be shown to be correlated to organic C, total N and cation exchange capacity. In addition, clay showed a weak positive correlation, while with sand, a negative correlation has been observed. No correlation was shown for pH, silt or $CaCO_3$ presence (Zantua et al., 1977). We could show that urease is also expressed in minimal medium, indicating a broader spectrum of inducers for the

enzyme and potentially wider substrate spectra linked to a possible role for biomineralization in natural soils.

We also could detect switzerite, a Mn-Fe phosphate (Fanfani and Zanazzi, 1979; Yakubovich et al., 2003), which in our case contained only Mn despite the presence of Fe in the media. Switzerite had been reported to be formed in the presence of the Gram-negative bacterium *Shewanella oneidensis* MR-1 under Fe(III)-reducing conditions, but with unknown genesis (Reardon et al., 2010). Here, we found several Gram-positive streptomycetes to be able to biomineralize switzerite. The role of the bacteria in formation of the mineral is evident from the finding that in all our assays, minerals were never formed on non-inoculated media or at larger distances from the colonies.

The green radial aggregates on TSB media spiked with $NiSO_4$ were identified as hydrated nickel hydrogen phosphate with the chemical formula $Ni(H_2O)_6HPO_4 \cdot H_2O$. The crystal structure of hexa-aqua-nickel(II) hydrogen phosphate monohydrate was published by Wang et al. (2005) after addition of $Ni(ClO_4)_2 \cdot H_2O$ to an aqueous solution of o-phospho-L-serine. However no biomineralization had been reported so far.

In this study, we have used sub-natural to natural conditions rather than soil extract to detect biominerals. It seems noteworthy that all three biominerals, all new at least for the genus *Streptomyces* which is dominant in our metal contaminated soil (Schütze and Kothe, 2012), were phosphates. In case of struvite precipitation, an external storage of P may be coupled to metal detoxification. Struvite has a very low solubility in water of about 160 $mg\,L^{-1}$ at 25 °C (Bhuiyan et al., 2007; Ohlinger et al., 1998; Kim et al., 2007). Since struvite is well soluble in an acidic environment (Hutnik et al., 2011) and streptomcetes are able to excrete acidic secondary metabolites (Bibb, 2005), they easily can (re)solubilize struvite, which is faster than for other phosphate minerals (Roncal-Herrero and Oelkers, 2011).

This study first showed biomineralization directly in soil and could show that streptomycetes are able to mineralize struvite independent of their metal resistance, whereas only heavy metal resistant streptomycetes have been involved in formation of switzerite and nickel hydrogen phosphate. Switzerite precipitation is first reported for the genus

Streptomyces. For mechanisms of biomineralization, in case of struvite, the excretion of secondary metabolites, pH changes induced and urease activity can be proposed as a mechanism with the potential benefit of remobilization and use of P, N and Mg. These findings may help to interpret the role of *Streptomyces* induced biomineralization and offer an explanation for biomineral formation in soil.

Supplementary material related to this article is available online at: http://www.biogeosciences-discuss.net/10/2345/2013/bgd-10-2345-2013-supplement.pdf.

Acknowledgements. We would like to thank HIGRADE and BMBF for funding, as well as JSMC and DFG-Gk1257 for support. Maria Wierzbicka-Wieczorek and Michael Abratis, Mineralogy, are thanked for introduction to EDX and XRR analysis. We also gratefully acknowledge the advice of Matthias Kästner from Environmental Biotechnology, Helmholtz Centre for Environmental Research – UFZ, Leipzig, Germany.

References

Adele, L. B.: Biomineralization: conflicts, challenges, and opportunities, J. Cell. Biochem., 72, 83–91, 1998.

Basnakova, G., Spencer, A. J., Palsgard, E., Grime, G. W., and Macaskie, L. E.: Identification of the nickel uranyl phosphate deposits on *Citrobacter* sp. cells by electron microscopy with electron probe X-ray microanalysis and by proton-induced X-ray emission analysis, Environ. Sci. Technol., 32, 760–765, 1998.

Ben Omar, N., Gonzalez-Munoz, M. T., and Penalver, J. M. A.: Struvite crystallization on *Myxococcus cells*, Chemosphere, 36, 475–481, 1998.

Bhuiyan, M. I., Mavinic, D. S., and Beckie, R. D.: A solubility and thermodynamic study of struvite, Environ. Technol., 28, 1015–1026, 2007.

Bibb, M. J.: Regulation of secondary metabolism in streptomycetes, Curr. Opin. Microbiol., 8, 208–215, 2005.

Chen, L., Shen, Y. H., Xie, A. J., Huang, F. Z., Zhang, W. Q., and Liu, S. X.: Seed-mediated synthesis of unusual struvite hierarchical superstructures using bacterium, Cryst. Growth Des., 10, 2073–2082, 2010.

Da Silva, S., Bernet, N., Delgenès, J. P., and Moletta, R.: Effect of culture conditions on the formation of struvite by *Myxococcus xanthus*, Chemosphere, 40, 1289–1296, 2000.

Doyle, J. D., Philp, R., Churchley, J., and Parsons, S. A.: Analysis of struvite precipitation in real and synthetic liquors, Process Saf. Environ., 78, 480–488, 2000.

Fanfani, L. and Zanazzi, P. F.: Switzerite – its chemical formula and crystal-structure, Miner. Petrol., 26, 255–269, 1979.

Gadd, G. M.: Metals, minerals and microbes: geomicrobiology and bioremediation, J. Med. Microbiol., 156, 609–643, 2010.

Gonzalez, H. and Jensen, T. E.: Nickel sequestering by polyphosphate bodies in *Staphylococcus aureus*, Microbios, 93, 179–185, 1998.

Haferburg, G., Kloess, G., Schmitz, W., and Kothe, E.: "Ni-struvite" – a new biomineral formed by a nickel resistant *Streptomyces acidiscabies*, Chemosphere, 72, 517–523, 2008.

Hesse, A., Schreyger, F., Tuschewitzki, G. J., Classen, A., and Bach, D.: Experimental investigations on dissolution of incrustations on the surface of catheters, Urol. Int., 44, 364–369, 1989.

Kamnev, A. A., Antonyuk, L. P., Colina, M., Cherynshev, A. V., and Ignatov, V. V.: Investigation of a microbially produced structural modification of magnesium-ammonium orthophosphate, Monatsh. Chem., 130, 1431–1442, 1999.

Kieser, T., Bibb, M. J., Buttner, M. J., Chater, K., and Hopwood, D. A.: Practical *Streptomyces* Genetics, The John Innes Foundation Norwich, England, 2000.

Kim, D., Ryu, H. D., Kim, M. S., Kim, J., and Lee, S. I.: Enhancing struvite precipitation potential for ammonia nitrogen removal in municipal landfill leachate, J. Hazard. Mater., 146, 81–85, 2007.

Kofina, A. N. and Koutsoukos, P. G.: Spontaneous precipitation of struvite from synthetic wastewater solutions, Cryst. Growth Des., 5, 489–496, 2005.

Konhauser, K. and Riding, R.: Bacterial biomineralization, in: Fundamentals of Geobiology, edited by: Knoll, A. H., Canfield, D. E., and Konhauser, K. O., John Wiley & Sons, Ltd, 105–130, 2012.

Le Corre, K. S., Valsami-Jones, E., Hobbs, P., and Parsons, S. A.: Impact of calcium on struvite crystal size, shape and purity, J. Cryst. Growth, 283, 514–522, 2005.

Le Corre, K. S., Valsami-Jones, E., Hobbs, P., and Parsons, S. A.: Impact of reactor operation on success of struvite precipitation from synthetic liquors, Environ. Technol., 28, 1245–1256, 2007a.

Le Corre, K. S., Valsami-Jones, E., Hobbs, P., and Parsons, S. A.: Kinetics of struvite precipitation: effect of the magnesium dose on induction times and precipitation rates, Environ. Technol., 28, 1317–1324, 2007b.

Lee, S. I., Weon, S. Y., Lee, C. W., and Koopman, B.: Removal of nitrogen and phosphate from wastewater by addition of bittern, Chemosphere, 51, 265–271, 2003.

McLean, R. J., Downey, J., Clapham, L., Wilson, J. W., and Nickel, J. C.: Pyrophosphate inhibition of *Proteus mirabilis*-induced struvite crystallization in vitro, Clin. Chim. Acta, 200, 107–117, 1991.

Ohlinger, K. N., Young, T. M., and Schroeder, E. D.: Predicting struvite formation in digestion, Water Res., 32, 3607–3614, 1998.

Párraga, J., Rivadeneyra, A. M., Martín-García, J. M., Delgado, R., and Delgado, G.: Precipitation of carbonates by bacteria from a saline soil, in matural and artificial soil extracts, Geomicrobiol. J., 21, 55–66, 2004.

Pérez-García, I., Rivadeneyra, M. A., and Ramos, C.: The influence of pH on struvite formation by bacteria, Chemosphere, 18, 1633–1638, 1989.

Prywer, J. and Torzewska, A.: Bacterially induced struvite growth from synthetic urine: experimental and theoretical characterization of crystal morphology, Cryst. Growth Des., 9, 3538–3543, 2009.

Prywer, J. and Torzewska, A.: Biomineralization of struvite crystals by *Proteus mirabilis* from artificial urine and their mesoscopic structure, Cryst. Res. Technol., 45, 1283–1289, 2010.

Reardon, C. L., Dohnalkova, A. C., Nachimuthu, P., Kennedy, D. W., Saffarini, D. A., Arey, B. W., Shi, L., Wang, Z., Moore, D., McLean, J. S., Moyles, D., Marshall, M. J., Zachara, J. M., Fredrickson, J. K., and Beliaev, A. S.: Role of outer-membrane cytochromes MtrC and OmcA in the biomineralization of ferrihydrite by *Shewanella oneidensis* MR-1, Geobiology, 8, 56–68, 2010.

Rivadeneyra, M. A., Calvo, C., González-Torres, M. C., Pérez-García, I., and Ramos-Cormenzana, A.: Precipitation of struvite in urine medium by urease-positive and urease-negative *Yersinia* strains, Urol. Int., 45, 298–301, 1990.

Rivadeneyra, M. A., Pérez-García, I., and Ramos-Cormenzana, A.: Struvite precipitation by soil and fresh water bacteria, Curr. Microbiol., 24, 343–347, 1992.

Rivadeneyra, M. A., Gutierrez-Calderón, A., Rivadeneyra, A. M., and Ramos-Cormenzana, A.: A study of struvite precipitation and urease activity in bacteria isolated from patients with urinary infections and their possible involvement in the formation of renal calculi, Urol. Int., 63, 188–192, 1999.

Roncal-Herrero, T. and Oelkers, E. H.: Experimental determination of struvite dissolution and precipitation rates as a function of pH, Appl. Geochem., 26, 921–928, 2011.

Ronteltap, M., Maurer, M., and Gujer, W.: The behaviour of pharmaceuticals and heavy metals during struvite precipitation in urine, Water Res., 41, 1859–1868, 2007.

Saidou, H., Korchef, A., Ben Moussa, S., and Ben Amor, M.: Struvite precipitation by the dissolved CO_2 degasification technique: impact of the airflow rate and pH, Chemosphere, 74, 338–343, 2009.

Schmidt, A., Haferburg, G., Sineriz, M., Merten, D., Büchel, G., and Kothe, E.: Heavy metal resistance mechanisms in actinobacteria for survival in AMD contaminated soils, Chem. Erde-Geochem., 65, 131–144, 2005.

Schmidt, A., Haferburg, G., Schmidt, A., Lischke, U., Merten, D., Ghergel, F., Büchel, G., and Kothe, E.: Heavy metal resistance to the extreme: *Streptomyces* strains from a former uranium mining area, Chem. Erde-Geochem., 69, 35–44, 2008.

Schütze, E. and Kothe, E.: Heavy metal-resistant streptomycetes in soil, in: Soil Biology, Springer-Verlag, Berlin Heidelberg, 2012.

Stefov, V., Soptrajanov, B., Kuzmanovski, I., Lutz, H. D., and Engelen, B.: Infrared and Raman spectra of magnesium ammonium phosphate hexahydrate (struvite) and its isomorphous analogues. III. Spectra of protiated and partially deuterated magnesium ammonium phosphate hexahydrate, J. Mol. Struct., 752, 60–67, 2005.

van Cappellen, P.: Biomineralization and global biogeochemical cycles, in: Biomineralization, edited by: Dove, P. M., Yoreo, J. J. D., and Weiner, S., Biogeochemistry of Earth Processes, Rev. Mineral. Geochem., 2003.

Veis, A.: Mineralization in an organic matrix framework, in: Biomineralization, edited by: Dove, P. M., Yoreo, J. J. D., and Weiner, S., Biogeochemistry of Earth Processes – Reviews in Mineralogy and Geochemistry, 2003.

Wang, X.-W., Wang II, P., and Zheng, Y.-Q.: Crystal structure of hexaaquanickel(II) hydrogenphosphate monohydrate, $[Ni(H_2O)_6][HPO_4] \times H_2O$, Z. Krist.–New Cryst. St., 220, 321–322, 2005.

Weiner, S. and Dove, P.: An overview of biomineralization and the problem of the vital effect, in: Biomineralization, edited by: Dove, P. M., Yoreo, J. J. D., and Weiner, S., Biogeochemistry of Earth Processes – Reviews in Mineralogy and Geochemistry, 2003.

Yakubovich, O. V., Massa, W., Soboleva, A. A., Dimitrova, O. V., and Urusov, V. S.: Crystal structure of a new synthetic homologue of the switzerite series, Dokl. Chem., 393, 262–269, 2003.

Zantua, M. I., Dumenil, L. C., and Bremner, J. M.: Relationships between soil urease activity and other soil properties, Soil Sci. Soc. Am. J., 41, 350–352, 1977.

Zeien, H. and Brümmer, G. W.: Chemische Extraktion zur Bestimmung der Schwermetallbindungsformen in Böden, Mitteilungen Deutschen Bodenkd. Ges., S. 59/I, 505–515, 1989.

Table 1. Growth and biomineralization under artificial conditions. The strains were grown on plates containing 1 mM of the indicated heavy metal for 56 days ($n = 3$).

		control		$AlCl_2$		$CuSO_4$		$MnCl_2$		$NiSO_4$		$ZnSO_4$		
genus	strain	TSB	AM	TSB	AM	TSB	AM	TSB	AM	TSB	AM	TSB	AM	
S. lividans	TK23	1	0	1	n.g.*	1	n.g.	1	n.g.	n.g.	n.g.	n.g.	n.g.	n.g.
S. acidiscabies	E13	1	0	1	n.g.	1	n.g.	1	2	n.g.	n.g.	n.g.	n.g.	n.g.
S. chromofuscus	P10A-4	1	0	1	n.g.	1	n.g.	1	2	3	0	n.g.	n.g.	
	P4B-1	1	0	1	n.g.	1	n.g.	1	0	0	0	0	0	
S. mirabilis	K7A-1	1	0	1	n.g.	1	n.g.	1	2	3	0	n.g.	0	
	P10A-3	1	0	1	n.g.	1	n.g.	1	0	3	0	n.g.	0	
	P16B-1	1	0	1	0	1	n.g.	1	0	3	0	0	0	
S. naganishii	P9A-1	1	0	1	n.g.	1	n.g.	1	2	3	0	0	0	
S. prunicolor	P6A-1	1	0	1	n.g.	1	n.g.	1	0	3	0	0	0	

Biominerals: 1, struvite; 2, switzerite; 3, nickel hydrogen phosphate; 0, no crytsals.
* n.g., no growth.

Table 2. Appearance of struvite crystal on TSB spiked with 1 mM metal salt.

genus	strain	$AlCl_2$	$CuSO_4$
S. lividans	TK23	radial aggregates of acicular crystals	no defined shape
S. acidiscabies	E13	acicular; grains, partly acicular	no defined shape
S. chromofuscus	P10A-4	close to colony: aggregates of grains; farther apart: radial aggregates of acicular crystals	no defined shape
	P4B-1	acicular; near colonies: parallel intergrowth of subhedral crystals	acicular, size negative correlated with distance to colony
	M2A-1	radial aggregates of acicular crystals; platy crystals with wedge-like outline; grains; acicular	no defined shape
S. mirabilis	P10A-3	at distance: radial aggregates of acicular crystals	at distance: radial aggregates of acicular crystals; aggregates of grains
	P16B-1	acicular; parallel intergrowth of subhedral crystals	acicular; aggregates of grains
S. naganishii	P9A-1	acicular; grains	radial aggregates of acicular crystals; acicular, grains; parallel intergrowth of subhedral crystals
S. prunicolor	P6A-1	no defined shape	parallel intergrowth of subhedral crystals

Table 3. CNS analysis of soil samples from contaminated sites (M2, M1) and control site (C).

	C	M1	M2
C_{total} [%]	8.55 ± 0.18	0.19 ± 0.03	4.05 ± 0.005
N [%]	0.58 ± 0.01	0.03 ± 0.00003	0.26 ± 0.007
S [%]	0.18 ± 0.004	n.d.*	0.17 ± 0.008

* not detectable.

Table 4. Growth and biomineralization under sub-natural conditions on soil agar (SA from M2, M1) after 56 days ($n = 3$).

		M1						M2								
genus	strain	TSB		AM		Con		TSB			AM			Con		
		a*	b	a	b	a	b	a	b	c	a	b	c	a	b	c
S. lividans	TK23	1	1	0	0	0	0	0	0	0	0	0	n.g.	0	0	0
S. acidiscabies	E13	1	0	0	n.g.	n.g.	n.g.	0	0	0	n.g.	n.g.	n.g.	0	n.g.	n.g.
S. chromofuscus	P10A-4	1	0	n.g.	0	n.g.	0	0	0	0	0	n.g.	0	0	0	0
	P4B-1	1	0	n.g.	0	n.g.	0	0	0	0	0	n.g.	0	0	0	0
S. mirabilis	K7A-1	1	1	n.g.	0	n.g.	0	0	0	0	0	0	0	0	0	0
	P10A-3	1	1	n.g.	0	n.g.	0	0	0	0	0	0	0	0	0	0
	P16B-1	1	1	n.g.	0	n.g.	0	0	0	0	0	0	0	0	0	0
S. naganishii	P9A-1	1	1	0	0	0	0	0	0	0	0	0	0	0	0	0
S. prunicolor	P6A-1	1	1	0	0	0	0	0	0	0	0	0	n.g.	0	0	0
S. tendae	F4	0	1	0	n.g.	0	n.g.	0	0	0	0	n.g.	n.g.	0	n.g.	n.g.

* soil dilution: a, 1 : 1; b, 1 : 5; c, 1 : 10.
n.g.: no growth after 56 days.
1: struvite formation; 0, no crytsals.

Table 5. Growth and biomineralization under natural conditions directly in soil with (M2, M1) or without metal contamination (C). The soil was nutrient enriched with either complex (TSB) or minimal (AM) medium, or left unamended with the respective amount of water added ($n = 3$).

genus	strain	C			M1			M2		
		TSB	AM	Con	TSB	AM	Con	TSB	AM	Con
S. lividans	TK23	2	0	0	1	n.g.*	n.g.	0	n.g.	n.g.
S. acidiscabies	E13	0	0	0	0	n.g.	n.g.	0	n.g.	0
S. chromofuscus	P10A-4	0	0	0	1	n.g.	n.g.	0	n.g.	0
	P4B-1	0	0	0	0	n.g.	n.g.	0	0	0
S.mirabilis	K7A-1	2	0	0	1	n.g.	1	0	n.g.	0
	P10A-3	1	0	0	0	n.g.	0	0	n.g.	0
	P16B-1	1	0	0	1	0	0	0	n.g.	0
S. naganishii	P9A-1	0	0	0	1	n.g.	n.g.	0	0	0
S.prunicolor	P6A-1	0	0	0	1	n.g.	0	0	n.g.	n.g.

Biominerals: 1: struvite; 2, switzerite; 3, nickel hydrogen phosphate; 0, no crystals.
* n.g., no growth.

Table 6. pH shift and ammonification in liquid AM (starting pH of 6) and TSB (starting pH of 7) after 7 days of growth.

genus	strain	TSB		AM	
		pH shift	NH_4	pH shift	NH_4
S. lividans	TK23	0.2	–	1.4	–
S. acidiscabies	E13	n.d.	–	−0.5	–
S. chromofuscus	P10A-4	2.7	+	0.8	–
S. mirabilis	P16A-1	0.1	–	−0.01	–
	P10A-3	2. 7	+	0.7	–
	P16B-1	2.2	+	0.5	–
S. naganishii	P9A-1	2.5	+	−1. 3	–
S. prunicolor	P6A-1	0.3	+	0.2	–
S. tendae	F4	n.d.	–	0.2	–

Ammonification: +: positive reaction; –: no reaction; no entry, ambiguous results.
pH shift: +: positive shift; –: negative shift; n.d.: not determined.

Table A1. Available metals [µg g^{-1} soil] of mobile (F1) and specifically adsorbed fraction (F2) from control soil (C) and heavy metal contaminated soils M1 and M2 measured by ESI ICP-MS, respectively ESI ICP-OES, ($n = 3$).

	M1 F1	M1 F2	C F1	C F2	M2 F1	M2 F2
Al	20.2 ± 0.2	0.9 ± 0.07	3.02 ± 0.07	31 ± 9	1.8 ± 0.07	14.2 ± 0.4
As	u.r.	u.r.	0.4 ± 0.07	0.5 ± 0.07	u.r.	u.r.
B	u.r.	u.r.	5.3 ± 0.2	2.4 ± 0.1	u.r.	u.r.
Ba	19.5 ± 0.005	1.6 ± 0.04	134.1 ± 0.02	66.8 ± 0.03	113 ± 2	71.1 ± 0.4
Ca	348 ± 5	13.9 ± 0.3	7011 ± 25	5067 ± 4	2033 ± 22	399 ± 3
Cd	0.04 ± 0.00002	u.r.	0.02 ± 0.005	0.2 ± 0.03	0.3 ± 0.007	1.4 ± 0.007
Co	2.4 ± 0.001	0.1 ± 0.007	0.1 ± 0.005	0.3 ± 0.01	2.9 ± 0.02	3.02 ± 0.001
Cr	0.03 ± 0.005	0.02 ± 0.0003	0.1 ± 0.01	0.3 ± 0.0001	0.02 ± 0.007	0.09 ± 0.01
Cu	0.6 ± 0.02	0.3 ± 0.04	1.1 ± 0.002	0.8 ± 0.004	8.1 ± 0.05	70.7 ± 0
Fe	30 ± 0.01	1.6 ± 0.1	4.2 ± 0.1	5.1 ± 0.2	u.r.	1.6 ± 0.002
K	64 ± 5	u.r.	154 ± 2	u.r.	56 ± 10	u.r.
Li	0.08 ± 0.01	0.1 ± 0.01	0.2 ± 0.02	0.1 ± 0.001	0.1 ± 0.01	0.2 ± 0.007
Mg	131 ± 0.7	6.8 ± 0.002	98.9 ± 0.002	490 ± 4	347 ± 2	32.1 ± 0.2
Mn	92.4 ± 0.2	4.3 ± 0.07	68.3 ± 0.2	161.3 ± 0.7	220 ± 1	99.7 ± 0.3
Na	4.9 ± 0.1	u.r.	6.8 ± 0.1	u.r.	22.9 ± 0.05	u.r.
Ni	1.8 ± 0.05	0.2 ± 0.04	0.2 ± 0.01	0.3 ± 0.04	2.6 ± 0.07	3.5 ± 0.1
P	u.r.	u.r.	16 ± 2	u.r.	u.r.	u.r.
Pb	0.1 ± 0.0005	0.2 ± 0.007	0.004 ± 0.0002	0.9 ± 0.03	u.r.	0.5 ± 0.007
S	10 ± 5	u.r.	75 ± 5	23.5 ± 0.1	327 ± 7	151.6 ± 0.3
Si	14.7 ± 0.5	12 ± 1	57 ± 2	138 ± 11	47 ± 1	46.1 ± 0.1
Sr	1.4 ± 0.01	0.09 ± 0.0007	47 ± 1	20.1 ± 0.2	15.2 ± 0.2	4.5 ± 0.002
Ti	u.r.	u.r.	u.r.	u.r.	u.r.	u.r.
V	u.r.	u.r.	0.2 ± 0.02	0.2 ± 0.02	u.r.	0.04 ± 0.01
Zn	0.9 ± 0.07	u.r.	u.r.	3.3 ± 0.2	10.05 ± 0.07	28.3 ± 0.3
Sc	u.r.	u.r.	u.r.	0.1 ± 0.02	u.r.	0.08 ± 0.02
Y	0.7 ± 0.02	0.3 ± 0.01	0.03 ± 0.002	0.09 ± 0.0007	0.02 ± 0.001	0.5 ± 0

* u.r.: under range

Table A1. Continued.

	M1 F1	M1 F2	C F1	C F2	M2 F1	M2 F2
Cs	u.r.	u.r.	u.r.	u.r.	0.04 ± 0.007	u.r.
La	0.3 ± 0.005	0.08 ± 0.003	0.02 ± 0.0007	0.06 ± 0.007	0.005 ± 0.00002	0.04 ± 0.0007
Ce	1.5 ± 0.01	0.5 ± 0.007	0.03 ± 0.002	0.1 ± 0.01	0.005 ± 0.001	0.09 ± 0.003
Pr	0.1 ± 0.002	0.05 ± 0.003	0.005 ± 0.0002	0.02 ± 0.002	u.r.	0.02 ± 0.001
Nd	0.5 ± 0.01	0.2 ± 0.003	0.02 ± 0.005	0.08 ± 0.004	0.005 ± 0.0007	0.1 ± 0.007
Sm	0.1 ± 0.002	0.09 ± 0.007	u.r.	0.02 ± 0.004	u.r.	0.05 ± 0.007
Eu	0.03 ± 0.00007	0.02 ± 0.002	0.001 ± 0.0005	0.004 ± 0.002	u.r.	0.02 ± 0.003
Tb	0.02 ± 0.0001	0.01 ± 0.0007	u.r.	0.004 ± 0.001	u.r.	0.01 ± 0
Gd	0.1 ± 0.005	0.1 ± 0.007	0.005 ± 0.001	0.03 ± 0.004	0.003 ± 0.00007	0.1 ± 0.004
Dy	0.1 ± 0.005	0.07 ± 0.0003	0.006 ± 0.0005	0.02 ± 0.002	0.002 ± 0.0002	0.06 ± 0.001
Ho	0.02 ± 0.001	0.01 ± 0.0007	0.001 ± 0.0001	0.004 ± 0.0004	u.r.	0.02 ± 0.00003
Er	0.05 ± 0.001	0.03 ± 0.0004	0.004 ± 0.0007	0.01 ± 0.003	u.r.	0.04 ± 0.002
Tm	0.006 ± 0.0002	0.004 ± 0.0003	u.r.	u.r.	u.r.	0.004 ± 0.0007
Yb	0.03 ± 0.002	0.02 ± 0.00004	0.003 ± 0.0007	0.008 ± 0.002	u.r.	0.02 ± 0.001
Lu	0.005 ± 0.0005	0.003 ± 0.0002	u.r.	u.r.	u.r.	0.004 ± 0.0004
Th	u.r.	u.r.	u.r.	0.009 ± 0.001	u.r.	u.r.
U	0.06 ± 0.002	0.7 ± 0.007	0.02 ± 0.001	0.04 ± 0.002	0.2 ± 0.001	171 ± 0.9

* u.r.: under range

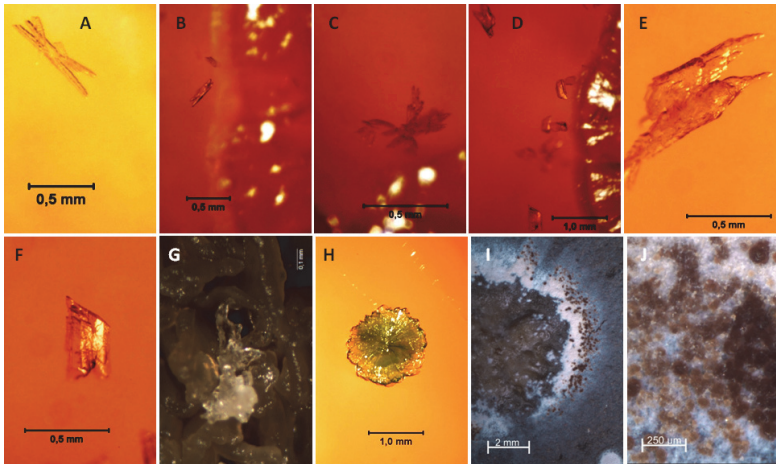

Fig. 1. Crystals mineralized in the presence of streptomycetes: assymmetric macroscopic structures of struvite **(A–F)** near colonies of *S. mirabilis* P16A-1 **(A–C)** and *S. acidiscabies* E13 **(E–F)**; encrusted mycelium of *S. acidiscabies* E13 **(G)**, nickel hydrogen phosphate (hydrated) of *S. chromofuscus* P10A-4 **(H)**; switzerite crystals of *S. acidiscabies* E13 **(I–J)**.

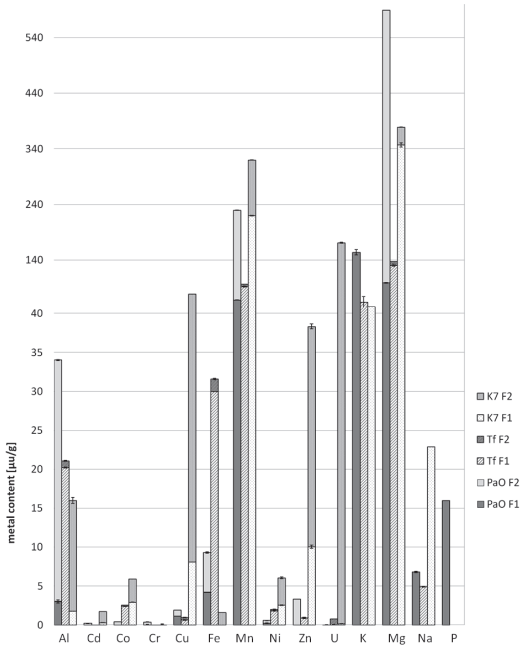

Fig. 2. Available metals and micronutrients [µg g^{-1} soil] of mobile fraction (F1) and specifically adsorbed fraction (F2) from control soil (C) and heavy metal contaminated soils M1 and M2.

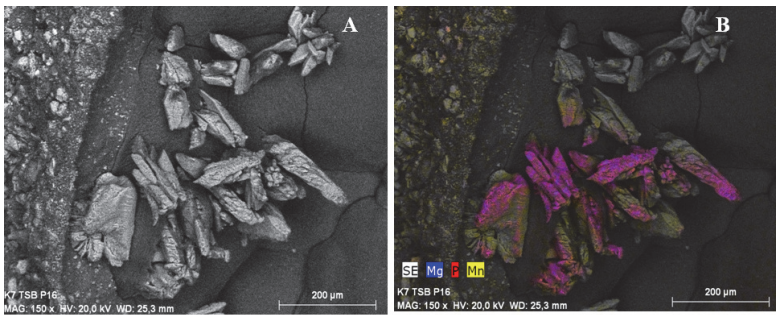

Fig. 3. Struvite crystals on the colony surface of *S. mirabilis* P16B-1: back scatter image **(A)**; corresponding element mapping **(B)**: blue, Mg; red, P; yellow, Mn; derived colour, elements corresponding to respective fast colours.

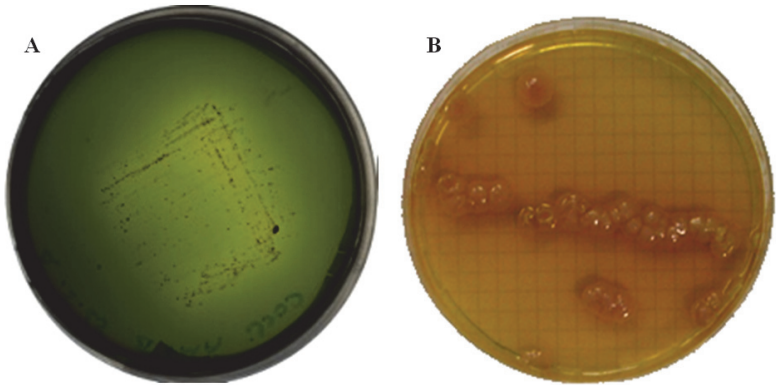

Fig. 4. Indicator plates display pH gradient due to bacterial inoculation after 7 days of growth: *S. lividans* TK23 on AM medium containing bromothymol blue **(A)**, neutral pH: green, acidic pH: yellow; *S. naganishii* P9A-1 on TSB medium containing methyl red **(B)**, neutral pH: yellow, basic pH: orange.

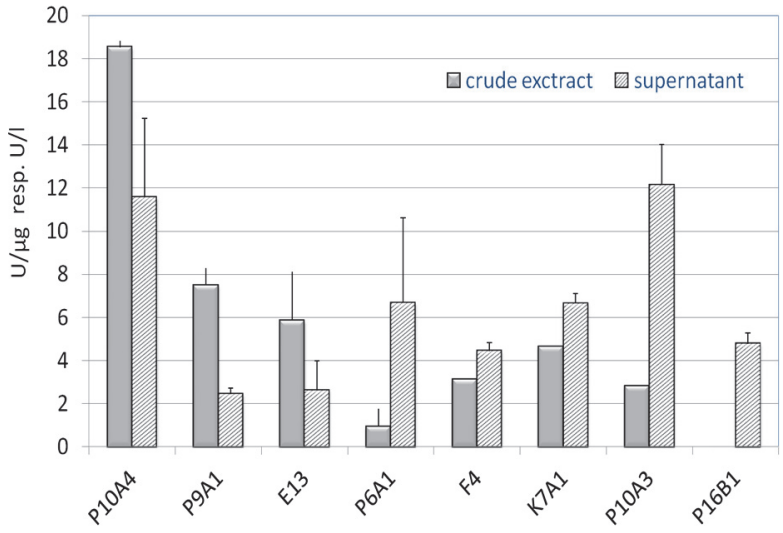

Fig. 5. Urease activity [$U\,L^{-1}$] in supernatant and specific activity [$U\,\mu g^{-1}$] in crude extract.